

High Performance Phase and Amplitude Modulators Based on GaInAsP Stepped Quantum Wells

*H. Mohseni, H. An, Z. A. Shellenbarger, M. H. Kwakernaak, and J. H. Abeles
Sarnoff Corporation, Princeton, NJ 08543-5300

ABSTRACT

Enhanced electrooptic coefficient of GaInAsP three-step quantum wells (3SQW) for high power electrorefraction modulator applications is reported. Measured electrooptic coefficient of the 3SQW is nearly three times higher than the conventional rectangular quantum well (RQW) at $\lambda=1.55\ \mu\text{m}$. Higher electrooptic effect, combined with a low optical absorption coefficient $\alpha < 1\ \text{cm}^{-1}$ in the 3SQW increased the modulator figure of merit by nearly 53 times, and decreased the power consumption by nearly one order of magnitude compared with a conventional RQW design.

Keyword: modulators, optical modulators, electrorefraction, compound semiconductors, quantum wells, stepped quantum wells.

1. INTRODUCTION

High-speed optical modulators are essential parts of most photonic systems. These devices are either based on electrorefraction (ER) or electroabsorption (EA). The former can be used for amplitude and phase modulation, while the latter can only be used for amplitude modulation. An inherent advantage of electrorefraction compared to electroabsorption is that the linear loss can be maintained very low. This leads to two important consequences. Low optical absorption leads to low electron-hole pair generation, as well as a low heat generation. Therefore, electrorefractive modulators can handle a much higher optical power densities compared to their electroabsorptive counterparts, due to the absence of bleaching and over heating. High optical power densities are extremely desirable for radio-frequency (RF) photonic and long-haul optical fiber communication systems. Moreover, a low optical absorption provides the possibility of using Fabry-Perot or ring resonator to form the so-called “slow-wave” modulation¹, where the modulation efficiency can be enhanced by orders of magnitude due to the enhanced interaction time.

Currently, the commonly used materials for high-speed phase modulators are lithium niobate (LN), III-V compound semiconductors, and polymers. Modulators based on LN have the most mature technology, since the material has been extensively studied for other commercial applications such as acoustic-wave filters for mobile phones. Traveling-wave LN modulators have achieved high bandwidths exceeding 100GHz^2 . Unfortunately, LN modulators cannot be integrated with III-V active components, and hence it is not a desirable material for the long sought realization of low-cost photonic subsystems with high functionality. Moreover, the inherently low electrooptic coefficient of lithium niobate $r_{33}\sim 30\text{pm/V}$, leads to a high operating voltage $V_{\pi}L=40$ to $80\ \text{Vmm}$, and consequently long device size and high power consumption.

Recently, polymeric modulators have been studied extensively. The main advantage of this type of modulators is their relatively easy fabrication process and a high modulation bandwidth exceeding $110\ \text{GHz}^3$. However, they have low electrooptic coefficients r_{33} in the 10 to 70 pm/V range, which combined with their low refractive index produces sensitivities similar to LN ($V_{\pi}L=30$ to $200\ \text{Vmm}$.) Other drawbacks of polymeric modulators include unproven lifetime and stability as well as limited maximum optical power density and operating temperature.

Although optical modulators based on III-V quantum wells have an inherently low operating voltage ($V_{\pi}L=10$ to $20\ \text{Vmm}$) compared to LN and polymeric modulators, they are difficult to couple to fiber optics and hence are not as suitable for discrete devices. However, they are excellent choices for monolithic integration with other III-V active and passive components. Power consumption becomes a much more

* Email: hmohseni@ieee.org

important issue for an integrated device, since power generation and transfer as well as heat dissipation are significantly restricted in a closely packed integrated subsystem. Therefore, there have been significant efforts to enhance the material sensitivity using novel quantum well designs.

Theoretically, more than one order of magnitude enhancement of sensitivity has been predicted for symmetric⁴ and asymmetric^{5,6,7,8} coupled quantum wells. Experimental results however, have shown enhancements approaching a factor of five⁹ in GaAs/AlGaAs material system. Unfortunately, such improvements have not been demonstrated for the InP based modulators, which are especially attractive for telecommunication applications. Here we report phase modulators employing InGaAsP/InP three-step quantum wells (3SQW) with nearly three times higher electrooptic coefficient compared to conventional rectangular quantum wells (RQW) at very low optical loss values. Stepped quantum wells, unlike coupled quantum wells, do not require very thin epitaxial layers or large change of material composition. Recent data¹⁰ indicates that even at the conventional growth temperature and duration, material interdiffusion can severely deform thin potential barriers. A high degree of interdiffusion in the GaInAsP material system may complicate the attainment of enhanced electrorefraction in the coupled quantum well approach.

2. MODELINGS AND EXPERIMENTS

We calculated optical absorption spectrum of the quantum wells using an effective mass approach. The excitonic effect was calculated based on a variational method⁶, and change of index was calculated from the Kramers-Kronig relationship. The electric field inside the active region was calculated using diffusion-drift and Poisson equations. Figure 1 shows the calculated wavefunctions and change of index for a given set of material composition and thickness.

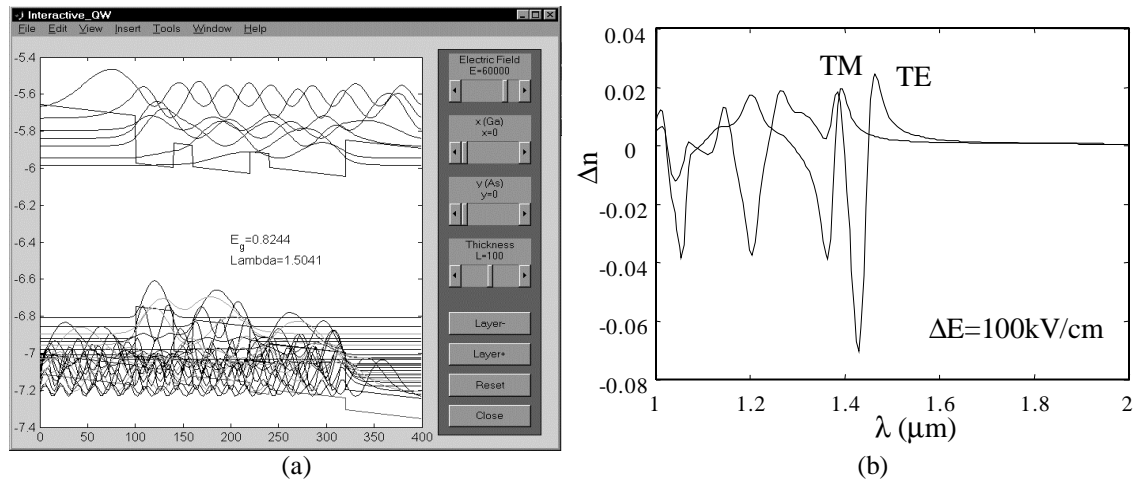
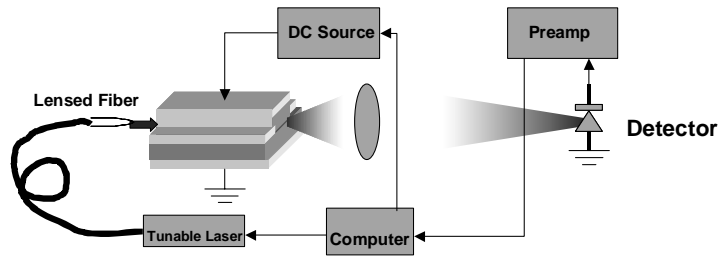
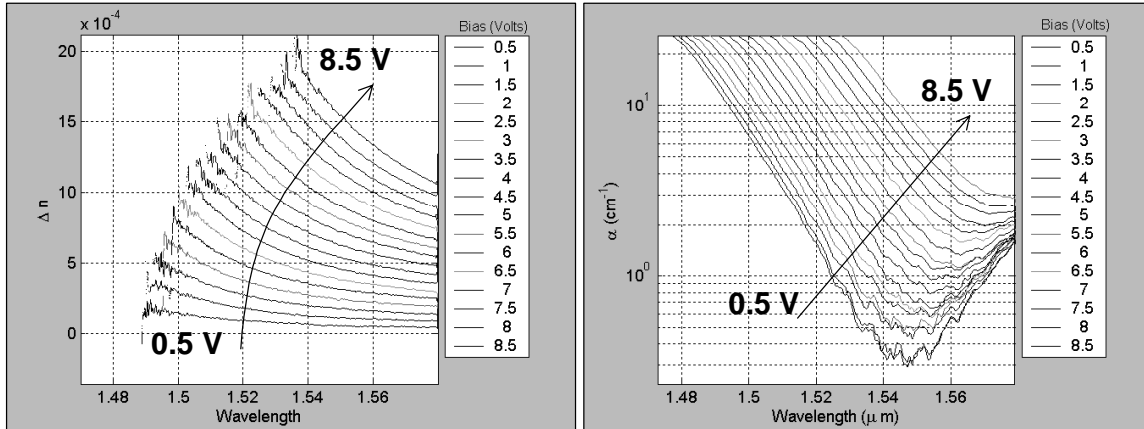


Figure 1: (a) Calculated electron and hole wavefunctions for a given set of material composition and thickness. (b) Calculated spectra of change of index for TE and TM modes under an external electric field of 100 kV/cm.

The thickness and composition of the layers of the quantum wells were optimized for a maximum change of index per change of voltage $\Delta n/\Delta V$, while keeping the absorption coefficient below $\alpha=1 \text{ cm}^{-1}$ at wavelengths near 1550 nm. Optimized quantum well structures were then grown by low-pressure metal organic vapor phase epitaxy (MOVPE) on n-type InP substrates. The active layers were $\sim 0.4 \mu\text{m}$ and were sandwiched between the $1.5 \mu\text{m}$ thick n and p-type InP cladding layers. The devices were terminated with a 50 nm thick, highly doped InGaAs cap layer. Structural and optical properties of the epitaxial layers were characterized with high-resolution x-ray diffraction and photoluminescence techniques. The material is then processed into single mode ridge waveguides through standard photolithography and wet or dry etching. We measured optical absorption coefficient and change of index of the modulators by measuring Fabry-Perot oscillation¹¹, optical transmission, and the modulator photoresponse. Figure 2-a shows the schematic of the measurement setup, while Figure 2-b and c show examples of the measured change of index and absorption coefficient spectra versus applied bias respectively.



(a)

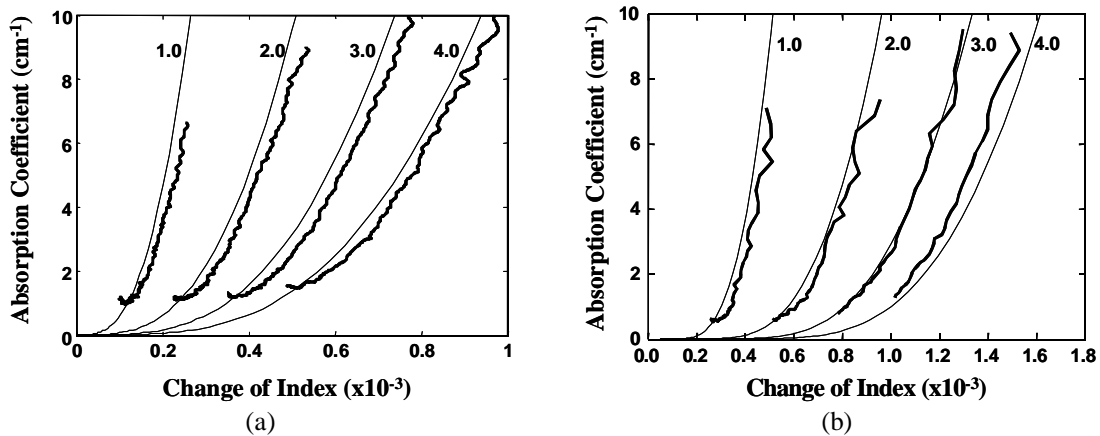


(b)

(c)

Figure 2: (a) Schematic of the measurement setup. (b) Measured spectra of change of index versus reverse bias voltage, and (c) measured optical absorption coefficient spectra versus reverse bias voltage.

Modeling data showed excellent agreement with measured data for modulators with conventional and stepped quantum active layers. Figure 3 compares the calculated and measured absorption coefficient versus change of index for modulators with two and three-step quantum wells. We believe that field-dependent excitonic broadening is the main reason for the deviation between the measured and modeled data at higher bias values.



(a)

(b)

Figure 3: Calculated (thin lines) and measured (thick lines) optical absorption coefficient versus the change of index for bias values between 1 to 4 volts for (a) a modulator with two-step quantum well active layer, and (b) a modulator with three-step quantum well active layer.

The performance of modulators with conventional rectangular quantum wells, and stepped quantum wells were compared systematically. Since the detuning from the energy gap of the devices has a significant effect on the measurement, we only compared devices with similar bandgap energies. Figure 4 compares the optical absorption coefficient versus change of index for a modulator with rectangular quantum well active region and a modulator with three-step quantum well active region. It is clear that the stepped quantum wells show much higher change of index per bias steps as well as much less increase in the optical loss. For reverse bias values below 4 volts, the modulator with stepped quantum well active layer shows nearly three times higher change of index per change of voltage than the modulator based on rectangular quantum well while the maximum optical absorption coefficient is about three times lower.

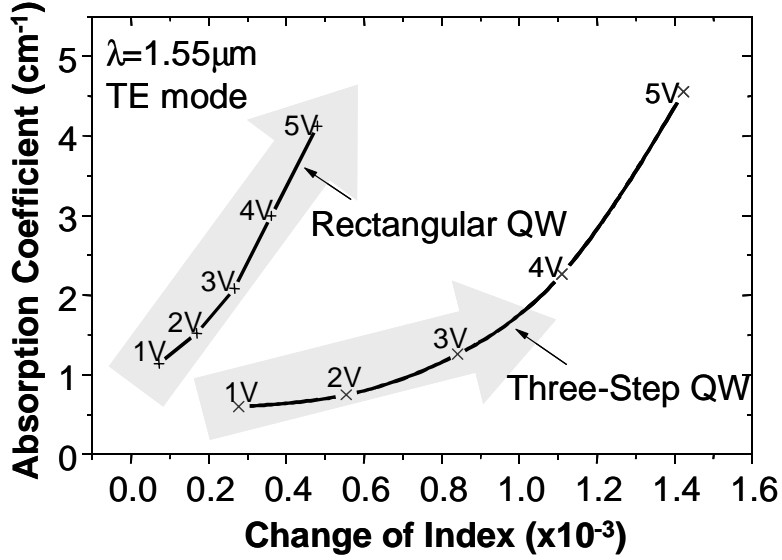


Figure 4: Optical absorption coefficient versus change of index of a modulator with conventional rectangular quantum well active region compared with a modulator with three-step quantum well active region. The former shows much higher change of index per bias steps as well as much less increase in the optical loss.

The importance of a low optical loss can be better understood by considering the gain of an impedance matched analog RF photonic link¹²:

$$G = \left(\frac{e^{-\alpha L}}{V_\pi} \cdot \frac{\pi 10^{-l/10} R r_d P}{4} \right)^2 \quad \text{Equation 1}$$

where α is the optical absorption coefficient, L is the length of the modulator, and V_π is the voltage required for a π phase shift, R is the detector responsivity, r_d is the detector resistance, P is the laser power, and l is the total loss from the interconnects and fiber optics in decibel. Retaining the relevant parameter to the modulator, one can define modulator figure of merit as $M = (\exp(-\alpha L)/V_\pi)^2$. Assuming a small change of index, the value of V_π can be calculated as $V_\pi = \lambda / [2L(\Delta n/\Delta V)]$. Here λ is the laser wavelength and $\Delta n/\Delta V$ is the change of index versus change of bias in the modulator. Therefore, the optimum length of the modulator required to maximize M can be calculated as $L_{opt} = 1/\alpha$ and the figure of merit of a modulator with the optimum length becomes:

$$M_{opt} = 4e^{-2} \left(\frac{\Delta n/\Delta V}{\alpha \lambda} \right)^2 \quad \text{Equation 2}$$

Table 1 compares the performance of modulators with conventional quantum well, two-step quantum well, and three-step quantum well active layers. The reduction of $V_{\pi}L$ product by nearly a factor of three for the three-step quantum well leads to significant enhancement of the modulator figure of merit.

Active Layer Structure	$\Delta n/\Delta V$ @ $V_{\text{bias}}=2$ volts (1/volt)	$V_{\pi}L$ (V.mm)	$(V_{\pi}L\alpha)^{-2} \propto$ Link Gain (V^{-2})
Rectangular QW	$\sim 1 \times 10^{-4}$	7.6	0.77
Two-step QW	$\sim 1.3 \times 10^{-4}$	5.8	2.97
Three-step QW	$\sim 3 \times 10^{-4}$	2.6	41.2

Table 1: Comparison of modulators with conventional quantum well, two-step quantum well, and three-step quantum well active layers.

3. CONCLUSION

In conclusion, we demonstrated InP based phase modulators based on stepped quantum wells with nearly three times higher $\Delta n/\Delta V$ compared with conventional rectangular quantum wells. Enhanced $\Delta n/\Delta V$ combined with an optical absorption coefficient below 1 cm^{-1} lead to ~ 17 dB higher link gain, and nearly one order of magnitude lower power consumption in the modulator. These properties make stepped quantum wells an excellent candidate for high-power, low-drive voltage MZ modulators required for high performance analog RF link applications.

4. ACKNOWLEDGEMENT

The authors would like to acknowledge the technical assistance of D. Capewell and L. Di Marco. This work is partially supported by DARPA/MTO under contract number F30602-00-C-0116.

REFERENCES

- ¹ H. Teylor, J. of Lightwave Technol. **17**, 1875 (1999).
- ² K. Noguchi, O. Mitomi, and H. Miyawaza, J. Lightwave Technol. **16**, 615 (1998).
- ³ D. Chen, H. Fetterman, A. Chen, W. Steier, L. Dalton, W. Wang, and Y. Shi, Appl. Phys. Lett **70**, 3335 (1997).
- ⁴ Y. Chan, and K. Tada, IEEE J. of Quantum Elect. **27**, 702 (1991).
- ⁵ H. Feng, J. Pang, K. Tada, and Y. Nakano, IEEE Photonic Technol. **9**, 639 (1997).
- ⁶ C. Thirstrup, IEEE J. of Quantum Elect. **31**, 988 (1995).
- ⁷ Y. Huang, Y. Chen, and C. Lien, Appl. Phys. Lett. **67**, 2603 (1995).
- ⁸ Y. Chen, H. Li, Z. Zhou, and K. Wang, J. Appl. Phys. **76**, 4903 (1994).
- ⁹ H. Feng, J. Pang, M. Sugiyama, K. Tada, and Y. Nakano, IEEE J. of Quantum. Elec. **34**, 1197 (1998).
- ¹⁰ J. Bursik, D. Malakhov, Y. Wang, G. Weatherly, and G. Purdy, J. of Applied Phys. **91**, 9613 (2002).
- ¹¹ T. R. Walker, Electron. Lett. **21**, 581 (1985).
- ¹² See for example S. Hamilton, D. Yankelevich, A. Knoesen, R. Weverka, and R. Hill, IEEE Transactions on Microwave Theory and Techniques **47**, 1184 (1999).